SUPPORTING INFORMATION

Supporting Figure Legends

Figure S1. Low-throughput assays of SLiM binding to six domains
(A) List of tested TNKS2^{ARC4}-binding peptides. K_D values are from [54].
(B) The experiment shown in Figure 2B was repeated using the transcriptional reporter, FUS1-lacZ (mean ± SD; n = 4).
(C) Comparison of the fold inhibition in FUS1-lacZ vs. P-MAPK assays, for all peptides in panel A. Both assays show affinity-dependent inhibition, but the P-MAPK assay detects weak binding with greater sensitivity. Fold inhibition (mean ± SD, n = 4) is the difference in signal between the test peptide and the control, as a fraction of the control signal. K_D values are mean ± SE [54].
(D) SLiM recognition by the Abp1^{SH3} domain, assayed using the FUS1-lacZ reporter. Bars, mean ± SD (n = 3). K_D values from [53].
(E) SLiM recognition by MDM2^{SWIB} and MDM4^{SWIB} domains, assayed as in Figure 2B. Bars, mean ± range (n = 2). K_D values from [33, 65].
(F) SLiM recognition by YAP^{WW1} and NEDD4^{WW3} domains, assayed as in Figure 2B. Bars, mean ± range (n = 2). Note that K_D values from distinct studies [55, 56] might not be directly comparable.
(G) Protein levels of GST-tagged Cln2 fusions expressed from promoters of different strengths (P_{GAL1}, P_{GALS}, P_{GALL}). Expression was induced with galactose for 105 min. G6PDH served as a loading control.

Figure S2. SIMBA interrogation of multiple TNKS2^{ARC4}-binding peptides
(A) SIMBA scores vs. K_D for all 3BP2 variants as well as variants at each of 8 individual positions, plotted as in Figure 3C, with the TNKS2^{ARC4}-Cln2 fusion driven by P_{GAL1} or P_{GALS}. All SIMBA scores are mean ± SEM (n = 4).
(B) Sequence and K_D of each motif subjected to DMS and SIMBA. Residues in the 8 core positions are colored where identical to (blue) or different from (orange) the 3BP2 sequence.
(C) Heatmaps of DMS results from six parent peptides, plotted as in Figure 3A.
(D) Distribution of SIMBA scores for all missense variants (black circles) and the average STOP codon (red X symbols) at the 12 positions in each of the 6 parent motifs.
(E) Correlation of SIMBA scores for variants inserted a the N-site vs. C-site locations, plotted as in Figure 3G, for six parent peptides.
(F) Correlation of SIMBA scores when the TNKS2^{ARC4}-Cln2 fusion was expressed from P_{GAL1} vs. P_{GALS}, plotted as in Figure 3F, for six parent peptides.
(G) Sequence preference logos, averaged from 5 motifs (excluding 3BP2-E5), comparing when the TNKS2^{ARC4}-Cln2 fusion was expressed from P_{GAL1} vs. P_{GALS}.

Figure S3. DMS data and characteristics of WW domain-binding peptides
(A) WW domain peptides used in this study, and their reported binding affinities. The consensus peptides (PYcon1-4) were designed based on “multiple PWM” sequences from Figure S1B of Ref [74], which were proposed as improved predictors of binding specificity compared to single PWMs.
(B) Heatmaps of DMS results for 12 peptides combined with 2 WW domains. Data are the mean of 3 independent replicate experiments.
(C) Conformations of WW domain bound peptides in published structures. The orientation is comparable to that in Figure 6G. PDB IDs: 4n7h, 2m3o, 2ez5, 5ydx, 2ltw.
(D) Plot of buried surface area (BSA) for residues in WW-bound peptides, expressed as a percentage of accessible surface area in the unbound peptide. Data are from 4 NEDD4^{WW3} complexes (all type 1) and 2 YAP^{WW1} complexes (type 2). Peptide names include PDB IDs.

Supporting Tables

Table S1. Yeast strains used in this study

Name	Relevant genotype *	Source
PPY2551	*MAT***a** *bar1Δ STE5-8A ste20Δ::kanMX6 HIS3::*P_{GAL1}*-GST-CLN2*	Ref. [20]
PPY2617	*MAT***a** *bar1Δ STE5-8A ste20Δ::kanMX6 FUS1::FUS1-lacZ::LEU2*	This study
PPY2622	*MAT***a** *bar1Δ STE5-8A ste20Δ::kanMX6 FUS1::FUS1-lacZ::LEU2 HIS3::*P_{GAL1}*-GST-MDM2*^{SWIB}*-CLN2*	This study
PPY2623	*MAT***a** *bar1Δ STE5-8A ste20Δ::kanMX6 FUS1::FUS1-lacZ::LEU2 HIS3::*P_{GAL1}*-GST-TNKS2*^{ARC4}*-CLN2*	This study
PPY2625	*MAT***a** *bar1Δ STE5-8A ste20Δ::kanMX6 FUS1::FUS1-lacZ::LEU2 HIS3::*P_{GALL}*-GST-MDM2*^{SWIB}*-CLN2*	This study
PPY2628	*MAT***a** *bar1Δ STE5-8A ste20Δ::kanMX6 FUS1::FUS1-lacZ::LEU2 HIS3::*P_{GALS}*-GST-MDM2*^{SWIB}*-CLN2*	This study
PPY2629	*MAT***a** *bar1Δ STE5-8A ste20Δ::kanMX6 FUS1::FUS1-lacZ::LEU2 HIS3::*P_{GALL}*-GST-TNKS2*^{ARC4}*-CLN2*	This study
PPY2631	*MAT***a** *bar1Δ STE5-8A ste20Δ::kanMX6 FUS1::FUS1-lacZ::LEU2 HIS3::*P_{GALS}*-GST-TNKS2*^{ARC4}*-CLN2*	This study
PPY2708	*MAT***a** *bar1Δ STE5-8A ste20Δ::kanMX6 FUS1::FUS1-lacZ::LEU2 HIS3::*P_{GAL1}*-GST-CLN2*	This study
PPY2727	*MAT***a** *bar1Δ STE5-8A ste20Δ::kanMX6 FUS1::FUS1-lacZ::LEU2 HIS3::*P_{GAL1}*-GST-YAP*^{WW1}*-CLN2*	This study
PPY2732	*MAT***a** *bar1Δ STE5-8A ste20Δ::kanMX6 FUS1::FUS1-lacZ::LEU2 HIS3::*P_{GAL1}*-GST-NEDD4*^{WW3}*-CLN2*	This study

* All strains in W303 background (*ADE2 his3-11,15 leu2-3,112 trp1-1 ura3-1 can1*)

Table S2. Plasmids used in this study

SUBSTRATE fusion plasmids

Name	Description	Peptide Motif Insert	Source
pPP4365	CEN URA3 myc13-(LP_Ste20 motif)-(Ste5 1-85)-(Ste20 312-939)	LP_Ste20 = VSLDDPIQFTA	Ref. [20]
pPP4366	CEN URA3 myc13-(LP_Ste5 motif)-(Ste5 1-85)-(Ste20 312-939)	LP_Ste5 = SPLLPPFGLSY	Ref. [20]
pPP4367	CEN URA3 myc13-(LP_Sic1 motif)-(Ste5 1-85)-(Ste20 312-939)	LP_Sic1 = EVLLPPSRPTS	Ref. [20]
pPP4368	CEN URA3 myc13-(LP_Whi5 motif)-(Ste5 1-85)-(Ste20 312-939)	LP_Whi5 = MPLLPPTTPKS	Ref. [20]
pPP4369	CEN URA3 myc13-(LP_Lam5 motif)-(Ste5 1-85)-(Ste20 312-939)	LP_Lam5 = KQLGPPFEHAS	Ref. [20]
pPP4375	CEN URA3 myc13-(nonLP_control motif)-(Ste5 1-85)-(Ste20 312-939)	nonLP = SNGNGSGSNGN	Ref. [20]
pPP4518	CEN URA3 myc13-(Amot_PY1 motif)-(Ste5 1-85)-(Ste20 312-939)	Amot_PY1 = NNEELPTYEEAK	This study
pPP4519	CEN URA3 myc13-(Amot_PY2 motif)-(Ste5 1-85)-(Ste20 312-939)	Amot_PY2 = HRGPPPEYPFKG	This study
pPP4521	CEN URA3 myc13-(PR_Ark1 motif)-(Ste5 1-85)-(Ste20 312-939)	PR_Ark1 = KKTKPTPPPKPSHLK	This study
pPP4522	CEN URA3 myc13-(PR_Prk1 motif)-(Ste5 1-85)-(Ste20 312-939)	PR_Prk1 = KSRPPRPPPKPLHLR	This study
pPP4523	CEN URA3 myc13-(PY_53BP2 motif)-(Ste5 1-85)-(Ste20 312-939)	PY_53BP2 = YPPYPPPPYPSG	This study
pPP4524	CEN URA3 myc13-(PY_Marburg motif)-(Ste5 1-85)-(Ste20 312-939)	PY_Marburg = MQYLNPPPYADH	This study
pPP4525	CEN URA3 myc13-(PY_Rabies motif)-(Ste5 1-85)-(Ste20 312-939)	PY_Rabies = DLWLPPPEYVPL	This study
pPP4526	CEN URA3 myc13-(REctrl motif)-(Ste5 1-85)-(Ste20 312-939)	REctrl = GSGSRLKPRGGN	This study
pPP4531	CEN URA3 myc13-(p53 motif)-(Ste5 1-85)-(Ste20 312-939)	p53 = SQETFSDLWKLLPEN	This study

pPP4532	CEN URA3 myc13-(p53-W23A motif)-(Ste5 1-85)-(Ste20 312-939)	p53-W23A = SQETFSDLAKLLPEN	This study
pPP4533	CEN URA3 myc13-(p53-P27A motif)-(Ste5 1-85)-(Ste20 312-939)	p53-P27A = SQETFSDLWKLLAEN	This study
pPP4534	CEN URA3 myc13-(NUMB motif)-(Ste5 1-85)-(Ste20 312-939)	NUMB = PVDPFEAQWAALENK	This study
pPP4536	CEN URA3 myc13-(3BP2 motif)-(Ste5 1-85)-(Ste20 312-939)	3BP2 = LQRSPPDGQSFR	This study
pPP4537	CEN URA3 myc13-(3BP2-E5 motif)-(Ste5 1-85)-(Ste20 312-939)	3BP2-D5E = LQRSPPEGQSFR	This study
pPP4538	CEN URA3 myc13-(3BP2-A5 motif)-(Ste5 1-85)-(Ste20 312-939)	3BP2-D5A = LQRSPPAGQSFR	This study
pPP4539	CEN URA3 myc13-(RPGopt motif)-(Ste5 1-85)-(Ste20 312-939)	RPGopt = LAREAGDGEEAR	This study
pPP4540	CEN URA3 myc13-(NUMA1 motif)-(Ste5 1-85)-(Ste20 312-939)	NUMA1 = LPRTQPDGTSVP	This study
pPP4541	CEN URA3 myc13-(MCL1 motif)-(Ste5 1-85)-(Ste20 312-939)	MCL1 = VARPPPIGAEVP	This study
pPP4649	CEN URA3 myc13-(3BP2-Q5 motif)-(Ste5 1-85)-(Ste20 312-939)	3BP2-D5Q = LQRSPPQGQSFR	This study
pPP4650	CEN URA3 myc13-(3BP2-S3 motif)-(Ste5 1-85)-(Ste20 312-939)	3BP2-P3S = LQRSSPDGQSFR	This study
pPP4651	CEN URA3 myc13-(3BP2-M3 motif)-(Ste5 1-85)-(Ste20 312-939)	3BP2-P3M = LQRSMPDGQSFR	This study
pPP4652	CEN URA3 myc13-(3BP2-A4 motif)-(Ste5 1-85)-(Ste20 312-939)	3BP2-P4A = LQRSPADGQSFR	This study
pPP4653	CEN URA3 myc13-(AXIN1 motif)-(Ste5 1-85)-(Ste20 312-939)	AXIN1 = APRPPVPGEEGE	This study
pPP4654	CEN URA3 myc13-(AXIN1-P2A motif)-(Ste5 1-85)-(Ste20 312-939)	AXIN1-P2A = APRAPVPGEEGE	This study
pPP4655	CEN URA3 myc13-(AXIN1-P3A motif)-(Ste5 1-85)-(Ste20 312-939)	AXIN1-P3A = APRPAVPGEEGE	This study
pPP4656	CEN URA3 myc13-(AXIN1-V4A motif)-(Ste5 1-85)-(Ste20 312-939)	AXIN1-V4A = APRPPAPGEEGE	This study
pPP4657	CEN URA3 myc13-(AXIN1-P5A motif)-(Ste5 1-85)-(Ste20 312-939)	AXIN1-P5A = APRPPVAGEEGE	This study
pPP4745	CEN URA3 myc13-(Ste20 1-86)-(Ste5 1-85)-(C3RE control motif)-(Ste20 312-939)	C3RE = DVCTPR	This study
pPP4747	CEN URA3 myc13-(Ste20 1-86)-(Ste5 1-85)-(LP_Ste5 motif)-(Ste20 312-939)	LP_Ste5 = SPLLPPFGLSYT	This study
pPP4748	CEN URA3 myc13-(Ste20 1-86)-(Ste5 1-85)-(Cnon2 control motif)-(Ste20 312-939)	Cnon2 = GSNGGSGSNGGS	This study
pPP4749	CEN URA3 myc13-(Ste20 1-86)-(Ste5 1-85)-(Cctrl control motif)-(Ste20 312-939)	Cctrl = GGSGGSGGSGGS	This study
pPP4750	CEN URA3 myc13-(Ste20 1-86)-(Ste5 1-85)-(LP_Ste20 motif)-(Ste20 312-939)	LP_Ste20 = VSLDDPIQFTRV	This study
pPP4751	CEN URA3 myc13-(Ste20 1-86)-(Ste5 1-85)-(LP_Lam5 motif)-(Ste20 312-939)	LP_Lam5 = KQLGPPFEHASN	This study
pPP4762	CEN URA3 myc13-(3BP2 motif)-(Ste5 1-85)-(Ste20 312-939)	3BP2 = ggsgLQRSPPDGQSFRggsg	This study
pPP4763	CEN URA3 myc13-(3BP2-D5E motif)-(Ste5 1-85)-(Ste20 312-939)	3BP2-D5E = ggsgLQRSPPEGQSFRggsg	This study
pPP4764	CEN URA3 myc13-(RPGopt motif)-(Ste5 1-85)-(Ste20 312-939)	RPGopt = ggsgLAREAGDGEEARggsg	This study
pPP4765	CEN URA3 myc13-(NUMA1 motif)-(Ste5 1-85)-(Ste20 312-939)	NUMA1 = ggsgLPRTQPDGTSVPggsg	This study
pPP4766	CEN URA3 myc13-(MCL1 motif)-(Ste5 1-85)-(Ste20 312-939)	MCL1 = ggsgVARPPPIGAEVPggsg	This study
pPP4767	CEN URA3 myc13-(AXIN1 motif)-(Ste5 1-85)-(Ste20 312-939)	AXIN1 = ggsgAPRPPVPGEEGEggsg	This study
pPP4768	CEN URA3 myc13-(Ste20 1-86)-(Ste5 1-85)-(3BP2 motif)-(Ste20 312-939)	3BP2-WT = ggsgLQRSPPDGQSFRggsg	This study
pPP4769	CEN URA3 myc13-(Ste20 1-86)-(Ste5 1-85)-(NUMA1 motif)-(Ste20 312-939)	NUMA1 = ggsgLPRTQPDGTSVPggsg	This study
pPP4836	CEN URA3 myc13-(p53 motif)-(Ste5 1-85)-(Ste20 312-939)	p53 = ggsgSQETFSDLWKLLPENggsg	This study
pPP4837	CEN URA3 myc13-(NUMB motif)-(Ste5 1-85)-(Ste20 312-939)	NUMB = ggsgPVDPFEAQWAALENKggsg	This study

CYCLIN fusion plasmids			
Name	**Description**	**Binding Domain Insert**	**Source**
pPP3573	CEN HIS3 Pgal1-GST-CLN2(1-372) Tcyc1	none	This study
pPP4517	CEN HIS3 Pgal1-GST-(YAP_WW1)-CLN2(1-372) Tcyc1	YAP_WW1 = aa 164-227	This study
pPP4520	CEN HIS3 Pgal1-GST-(Abp1_SH3)-CLN2(1-372) Tcyc1	Abp1_SH3 = aa 535-592	This study
pPP4527	CEN HIS3 Pgal1-GST-(NEDD4_WW3)-CLN2(1-372) Tcyc1	NEDD4_WW3 = aa 834-878	This study
pPP4542	CEN HIS3 Pgal1-GST-(TNKS2_ARC4)-CLN2(1-372) Tcyc1	TNKS2_ARC4 = aa 488-649	This study
pPP4543	CEN HIS3 Pgal1-GST-(MDM2_SWIB)-CLN2(1-372) Tcyc1	MDM2_SWIB = aa 17-109	This study
pPP4544	CEN HIS3 Pgal1-GST-(MDM4_SWIB)-CLN2(1-372) Tcyc1	MDM4_SWIB = aa 24-108	This study
pPP4575	integrating HIS3 Pgal1-GST-(MDM2_SWIB)-CLN2(1-545) Tcyc1	MDM2_SWIB = aa 17-109	This study
pPP4576	integrating HIS3 Pgal1-GST-(TNKS2_ARC4)-CLN2(1-545) Tcyc1	TNKS2_ARC4 = aa 488-649	This study
pPP4643	integrating HIS3 PgalL-GST-(MDM2_SWIB)-CLN2(1-545) Tcyc1	MDM2_SWIB = aa 17-109	This study
pPP4644	integrating HIS3 PgalS-GST-(MDM2_SWIB)-CLN2(1-545) Tcyc1	MDM2_SWIB = aa 17-109	This study
pPP4659	integrating HIS3 PgalL-GST-(TNKS2_ARC4)-CLN2(1-545) Tcyc1	TNKS2_ARC4 = aa 488-649	This study
pPP4660	integrating HIS3 PgalS-GST-(TNKS2_ARC4)-CLN2(1-545) Tcyc1	TNKS2_ARC4 = aa 488-649	This study
pPP4866	integrating HIS3 Pgal1-GST-(YAP_WW1)-CLN2(1-545) Tcyc1	YAP_WW1 = aa 164-227	This study
pPP4867	integrating HIS3 Pgal1-GST-(NEDD4_WW3)-CLN2(1-545) Tcyc1	NEDD4_WW3 = aa 834-878	This study

Figure S1

A

motif	sequence	K_D:TNKS2^{ARC4}
3BP2	LQ**RSPPDG**QSFR	3.8 μM
3BP2-D5E	LQ**RSPPEG**QSFR	22.0 μM
3BP2-D5A	LQ**RSPPAG**QSFR	70.0 μM
3BP2-D5Q	LQ**RSPPQG**QSFR	46.4 μM
3BP2-P3S	LQ**RSSPDG**QSFR	7.9 μM
3BP2-P3M	LQ**RSMPDG**QSFR	11.9 μM
3BP2-P4A	LQ**RSPADG**QSFR	8.8 μM
RPGopt	LA**REAGDG**EEAR	0.6 μM
NUMA1	LP**RTQPDG**TSVP	17.2 μM
MCL1	VA**RPPPIG**AEVP	2.4 μM
AXIN1	AP**RPPVPG**EEGE	6.5 μM
AXIN1-P2A	AP**RAPVPG**EEGE	34.2 μM
AXIN1-P3A	AP**RPAVPG**EEGE	12.3 μM
AXIN1-V4A	AP**RPPAPG**EEGE	29.9 μM
AXIN1-P5A	AP**RPPVAG**EEGE	19.9 μM

B

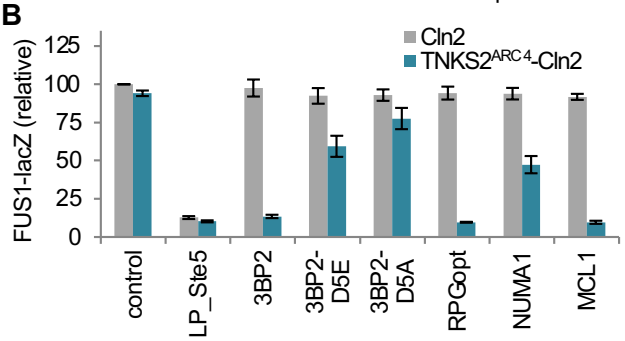

C

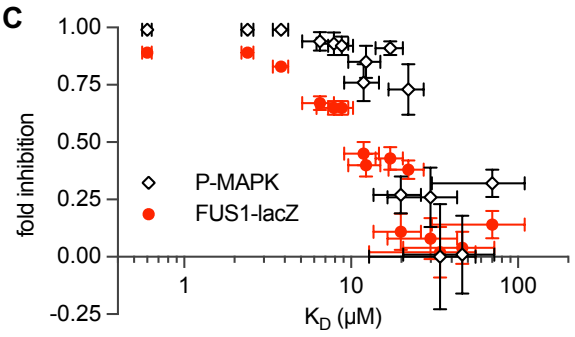

D

motif	sequence	K_D:Abp1^{SH3} 17-mer	15-mer
PR_Ark1	KKTK**P**TPP**P**K**P**SHLK	0.27 μM	0.77 μM
PR_Prk1	KSRP**P**RPP**P**K**P**LHLR	0.21 μM	?

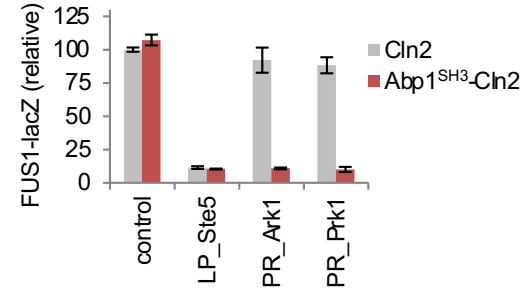

E

motif	sequence	K_D:MDM2^{SWIB}	K_D:MDM4^{SWIB}
p53-WT	SQET**FSDLWKLL**PEN	0.4 μM	0.6 μM
p53-W23A	SQET**FSDLAKLL**PEN	defective	defective
p53-P27A	SQET**FSDLWKLLA**EN	0.05 μM	0.2 μM
NUMB	PVDP**FEAQWAAL**ENK	3.3 μM	?

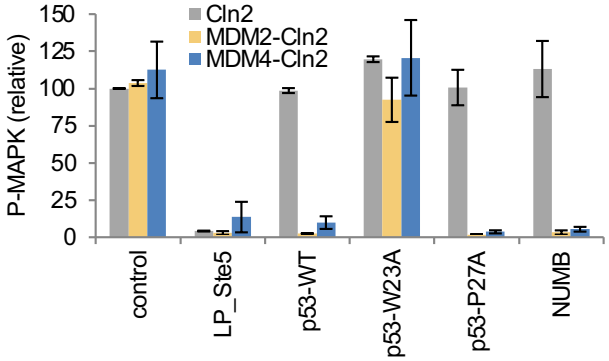

F

motif	sequence	K_D:YAP^{WW1}	K_D:NEDD4^{WW3}
PY1_Amot	NNEE**LPTY**EEAK	7.1 μM	?
PY2_Amot	HRGP**PPEY**PFKG	6.6 μM	?
PY_53BP2	YPPYP**PPPY**PSG	1.8 μM	5.3 μM
PY_Marburg	MQYLN**PPPY**ADH	67 μM	51 μM
PY_Rabies	DLWLP**PPEY**VPL	181 μM	51 μM

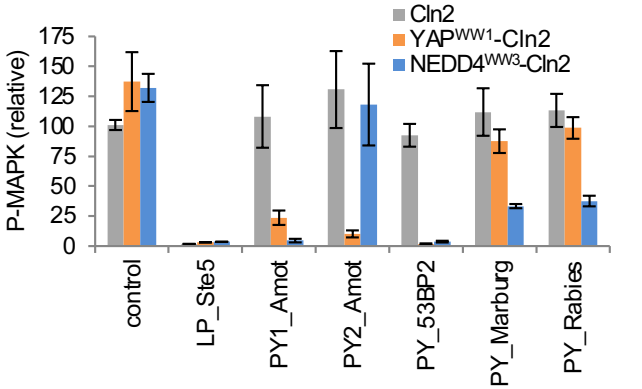

G

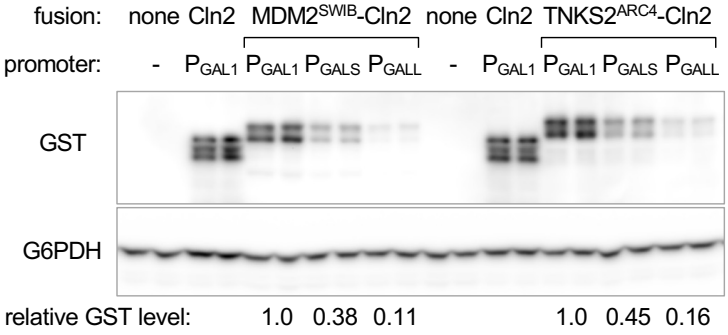

Figure S1. Low-throughput assays of SLiM binding to six domains

(**A**) List of tested TNKS2^{ARC4}-binding peptides. K_D values are from [54]. (**B**) The experiment shown in Figure 2B was repeated using the transcriptional reporter, FUS1-lacZ (mean ± SD; n = 4). (**C**) Comparison of the fold inhibition in FUS1-lacZ vs. P-MAPK assays, for all peptides in panel A. Both assays show affinity-dependent inhibition, but the P-MAPK assay detects weak binding with greater sensitivity. Fold inhibition (mean ± SD, n = 4) is the difference in signal between the test peptide and the control, as a fraction of the control signal. K_D values are mean ± SE [54]. (**D**) SLiM recognition by the Abp1^{SH3} domain, assayed using the FUS1-lacZ reporter. Bars, mean ± SD (n = 3). K_D values from [53]. (**E**) SLiM recognition by MDM2^{SWIB} and MDM4^{SWIB} domains, assayed as in Figure 2B. Bars, mean ± range (n = 2). K_D values from [33, 65]. (**F**) SLiM recognition by YAP^{WW1} and NEDD4^{WW3} domains, assayed as in Figure 2B. Bars, mean ± range (n = 2). Note that K_D values from distinct studies [55, 56] might not be directly comparable. (**G**) Protein levels of GST-tagged Cln2 fusions expressed from promoters of different strengths (P_{GAL1}, P_{GALS}, P_{GALL}). Expression was induced with galactose for 105 min. G6PDH served as a loading control.

Figure S2

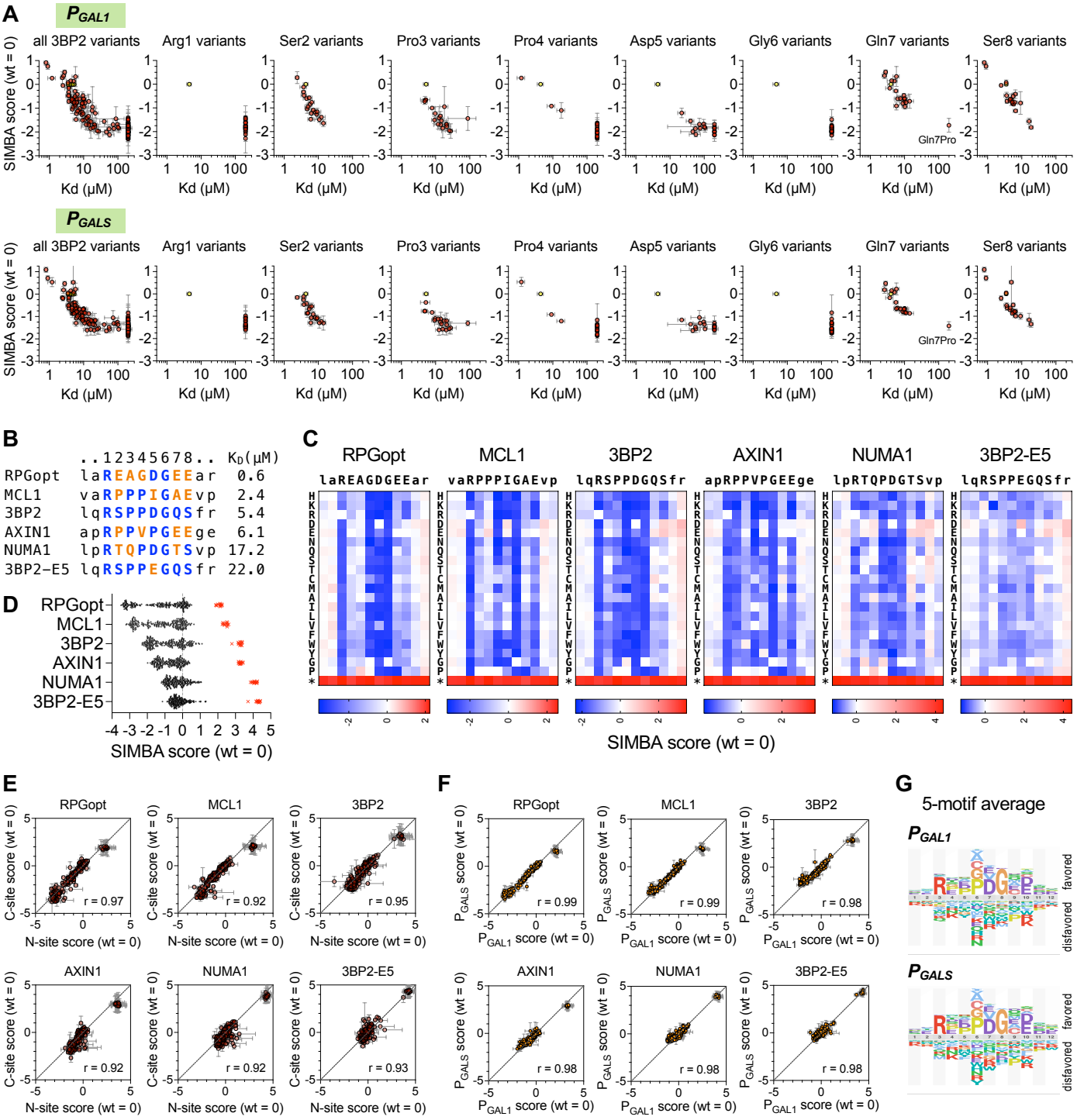

Figure S2. SIMBA interrogation of multiple TNKS2^{ARC4}-binding peptides

(**A**) SIMBA scores vs. K_D for all 3BP2 variants as well as variants at each of 8 individual positions, plotted as in Figure 3C, with the TNKS2^{ARC4}-Cln2 fusion driven by P_{GAL1} or P_{GALS}. All SIMBA scores are mean ± SEM (n = 4). (**B**) Sequence and K_D of each motif subjected to DMS and SIMBA. Residues in the 8 core positions are colored where identical to (blue) or different from (orange) the 3BP2 sequence. (**C**) Heatmaps of DMS results from six parent peptides, plotted as in Figure 3A. (**D**) Distribution of SIMBA scores for all missense variants (black circles) and the average STOP codon (red X symbols) at the 12 positions in each of the 6 parent motifs. (**E**) Correlation of SIMBA scores for variants inserted a the N-site vs. C-site locations, plotted as in Figure 3G, for six parent peptides. (**F**) Correlation of SIMBA scores when the TNKS2^{ARC4}-Cln2 fusion was expressed from P_{GAL1} vs. P_{GALS}, plotted as in Figure 3F, for six parent peptides. (**G**) Sequence preference logos, averaged from 5 motifs (excluding 3BP2-E5), comparing when the TNKS2^{ARC4}-Cln2 fusion was expressed from P_{GAL1} vs. P_{GALS}.

Figure S3

A

Peptide Category	Motif	Sequence *	Reported K_D (μM) †		Refs. ‡
			YAP^{WW1}	NEDD4^{WW3}	
(i) natural	AmotPY1	NNEELPTYEEAK	7.1	NR	1
	AmotPY1b	NEELPTYEEAKV	7.1	NR	1
	AmotPY2	HRGPPPEYPFKG	6.6	NR	1
	Smad7	LESPPPPYSRYP	6.9	8.0	2
	Lats1PY1	NRQPPPPYPLTA	15	NR	3
	Lats1PY2	YQGPPPPYPKHL	4.2	NR	3
	aENaC	LTAPPPAYATLG	NR	10	4
	bENaC	PGTPPPNYDSLR	NR	14	4
	Comm	IATGLPSYDEAL	NR	3.1	5
	ARRDC3	RPEAPPSYAEVV	NR	3.3	6
	53BP2	PPYPPPPYPSGE	1.8	5.3	7
	Marburg	QYLNPPPYADHG	67	51	7
	Rabies	LWLPPPEYVPLK	181	51	7
	Ebola	LPTAPPEYMEAI	750	76–147	7,8
	HTLV1	SDPQIPPPYVEP	61	308	7
(ii) optimized	UGR2	LDSLPSYSELFP	NR	0.15	8
	UGR1	LDAPPSYSELFP	NR	0.15	8
	UGR1-LYG	LDAPPSYSELYG	NR	0.92	8
(iii) consensus	PYcon1	AVPPNYSELFAT	NR	NR	
	PYcon2	TLPPPYSSYCMT	NR	NR	
	PYcon3	AVLPDYVTAMWQ	NR	NR	
	PYcon4	SKLPSYWFWRAN	NR	NR	

* Sequences tested in this study; some sequences tested in previous studies differ in length or boundaries.

† Values from different studies and methods may not be directly comparable. NR, not reported.

‡ References – PMIDs: (1)23564455; (2)22921829; (3)29487715; (4)12654927; (5)16531238; (6)24379409; (7)31636332; (8)35257734

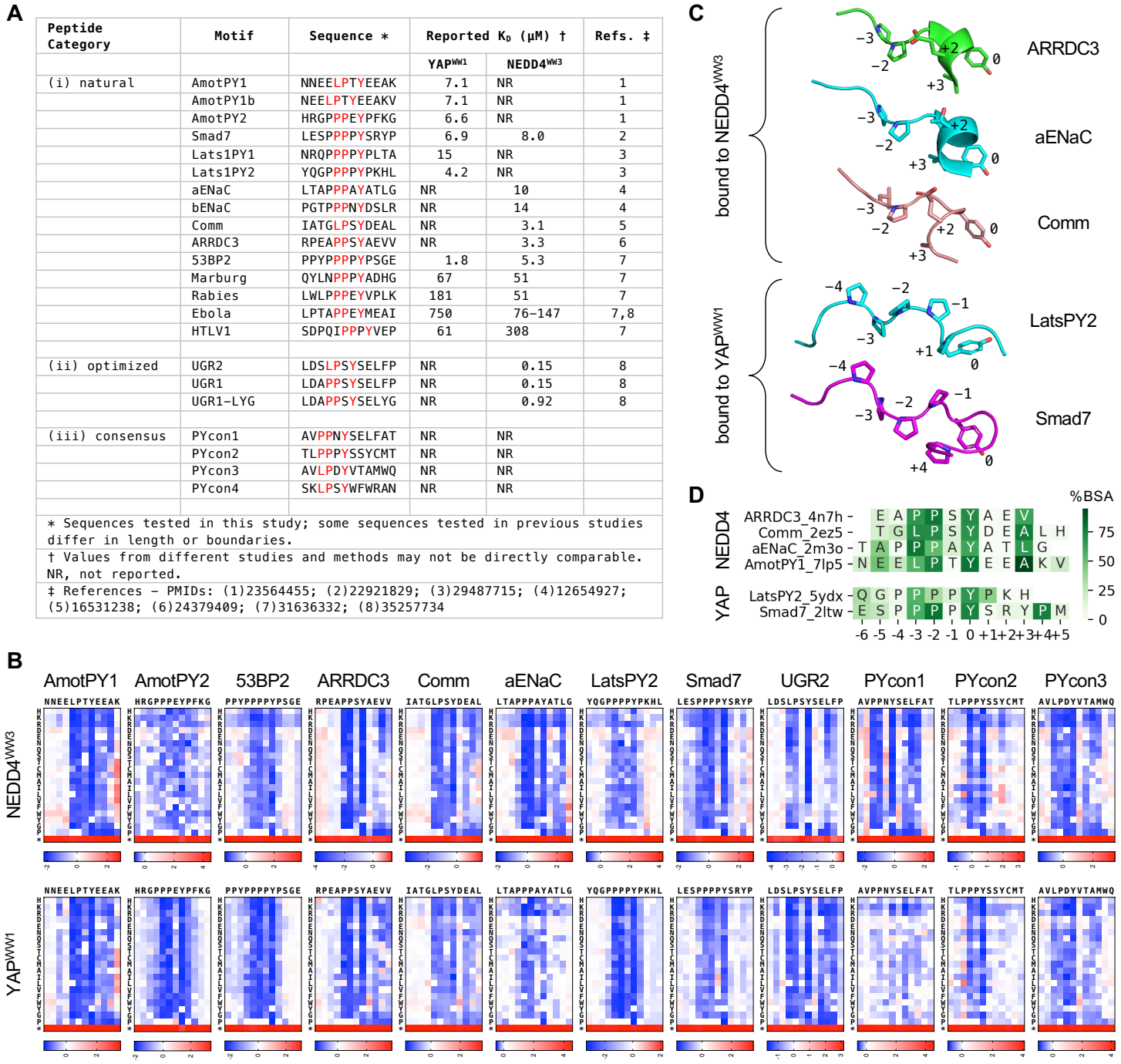

Figure S3. DMS data and characteristics of WW domain-binding peptides

(**A**) WW domain peptides used in this study, and their reported binding affinities. The consensus peptides (PYcon1-4) were designed based on "multiple PWM" sequences from Figure S1B of Ref [74], which were proposed as improved predictors of binding specificity compared to single PWMs. (**B**) Heatmaps of DMS results for 12 peptides combined with 2 WW domains. Data are the mean of 3 independent replicate experiments. (**C**) Conformations of WW domain bound peptides in published structures. The orientation is comparable to that in Figure 6G. PDB IDs: 4n7h, 2m3o, 2ez5, 5ydx, 2ltw. (**D**) Plot of buried surface area (BSA) for residues in WW-bound peptides, expressed as a percentage of accessible surface area in the unbound peptide. Data are from 4 NEDD4^{WW3} complexes (all type 1) and 2 YAP^{WW1} complexes (type 2). Peptide names include PDB IDs.